Self-assembly of colloidal polymers via depletion-mediated lock and key binding

Douglas J. Ashton, Robert L. Jack, and Nigel B. Wilding
Department of Physics, University of Bath, Bath BA2 7AY, United Kingdom

We study the depletion-induced self-assembly of indented colloids. Using state-of-the-art Monte Carlo simulation techniques that treat the depletant particles explicitly, we demonstrate that colloids assemble by a lock-and-key mechanism, leading to colloidal polymerization. The morphology of the chains that are formed depends sensitively on the size of the colloidal indentation, with smaller values additionally permitting chain branching. In contrast to the case of spheres with attractive patches, Wertheim's thermodynamic perturbation theory fails to provide a fully quantitative description of the polymerization transition. We trace this failure to a neglect of packing effects and we introduce a modified theory that accounts better for the shape of the colloids, yielding improved agreement with simulation.

The goal of self-assembly is to tailor the interactions among nano-scale particles so that they spontaneously assemble themselves into functional materials or devices [1, 2]. Such processes are widespread in biology, where they have been optimised by evolution so that assembly is rapid and reliable. However, mimicking this behaviour in the laboratory involves many challenges, particularly the design and synthesis of particles whose interactions can be accurately predicted and controlled. Notable experimental successes have included assembly of unusual crystals from either "patchy" or DNA-functionalised colloids [3, 4]. More recently, particles have been shown to self-assemble into structures that depend strongly on their *geometrical shapes* [5–9], and the role of shape and packing effects in self-assembly has also attracted theoretical and computational interest [7–12]. Here, we use computer simulations to show how self-assembly of indented colloidal particles can be tuned by subtly varying their shape and interactions, in a manner that should be accessible in experiment [6].

To this end, we exploit *depletion forces* [13], which enable the precise control of particle interactions that is required for self-assembly. Depletion is an attractive interaction between colloid particles that arises when they are mixed with much smaller 'depletant' particles, for example polymers or another species of colloid. These forces are particularly strong in colloids with complementary geometrical forms, such as buckled spheres [6] or bowl shapes [7]. Such systems can assemble via "lock and key binding" in which the convex part of one particle interlocks with the concave part of another [6, 11, 14]. Fig. 1 shows the results of a computer simulation, where colloids with self-complementary shapes [6] have assembled themselves into chains, in the presence of depletant particles. We show in the following that the properties of these "colloidal polymers" can be controlled through the colloidal shape and the depletant number density. The persistence length of the polymer depends on the colloidal shape, and for some shapes, the chains can also branch, leading to the possibility of "empty liquid" states [15, 16].

We emphasize that the complementary shapes of colloidal particles [6, 17, 18] and properties of the depletion interaction can both be measured and controlled in experiments. Indeed, some depletants even allow colloid interactions to be tuned *in situ* [5, 19, 20], potentially leading to real-time adaptive control of interaction parameters [21]. However, the experimental parameter space associated with mixtures of colloid and depletant particles is very large, depending on the size, shape and concentration of both species. Theory and computer simulation can therefore offer guidance for experiment, by predicting the parameters for which robust assembly occurs, and the likely nature of the self-assembled products. We argue that such simulations should deal explicitly with the depletant particles, both in the interests of reproducing the experimental reality and for avoiding the need to develop effective ("depletion") potentials, which for irregularly shaped particles represents a formidable task.

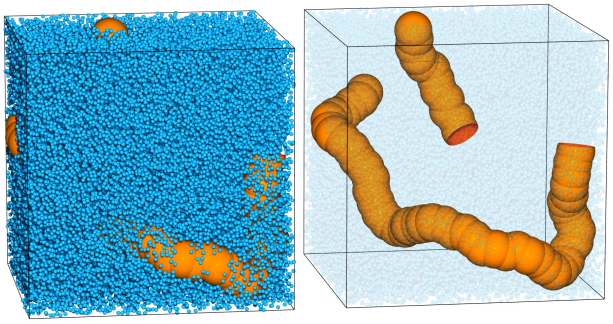

FIG. 1: (Color online) Equilibrium snapshot of self-assembled chains of spherically-indented colloids. The depletant is shown explicitly in the left panel but suppressed in the right panel, for clarity. System parameters are $h = 0.7$ and $\eta_s^r = 0.094$: see text for details.

Thus, we have deployed state-of-the-art Monte Carlo (MC) simulation techniques to study spherically-indented colloids, together with smaller hard sphere particles which act as a depletant. The shape of each indented colloid begins as a hard sphere of diameter $\sigma_l = 1$, from which an indentation is formed by cutting away a sphere of the same diameter, whose center is a distance d_c from the center of the original sphere. Thus, the di-

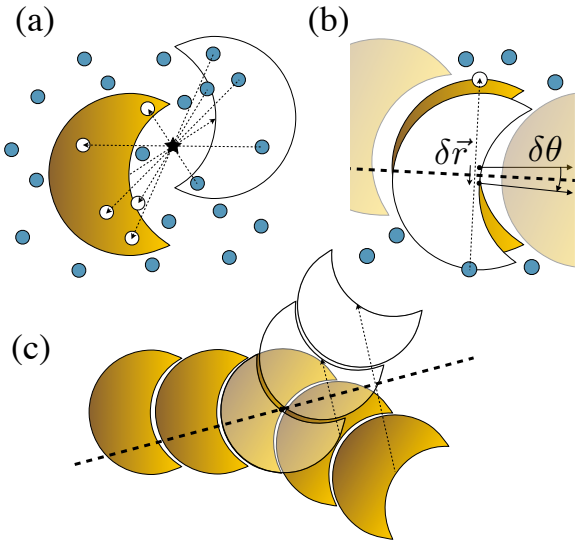

FIG. 2: (Color online) GCA move set for indented particles. **(a)** A colloid reflects through a point pivot to a new position (outlined). Any particles that overlap in the new position reflect through the same pivot to occupy the space vacated by the colloid. **(b)** Constrained plane reflections (see text) allow for small scale vibrations of colloids within a chain. **(c)** Reflecting a colloid in a plane passing through its center moves it to a new position (outlined). When overlapping particles are similarly reflected, the chain 'flexes'.

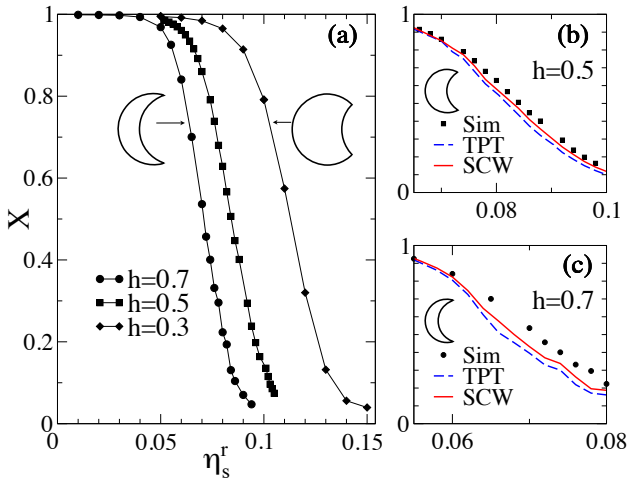

FIG. 3: (Color online)**(a)** Simulation estimates of $X(\eta_s^r)$ for $h = 0.3, 0.5, 0.7$; lines are guides to the eye and uncertainties are comparable to the symbol sizes. Comparison of the simulation data (Sim) with the predictions of TPT and SCW (see text) in the non-branching regime **(b)** $h = 0.7$, and **(c)** $h = 0.5$. There are numerical uncertainties in the TPT/SCW predictions which are comparable with those in the simulation data: these arise from the numerical estimation of f_A from simulations containing two colloids with depletant.

mensionless depth of the indentation is $h \equiv 1 - d_c/\sigma_l$. Our systems contain $N = 60$ colloid particles in a box of size V, with a number density $\rho = N/V = 0.2\sigma_l^{-3}$ and we consider values of h between 0.3 and 0.7. The hard spheres comprising the depletant fluid have diameter $\sigma_s = 0.1\sigma_l$. The colloid shape and the size ratio between colloids and depletant are consistent with experimental studies such as [6].

To obtain accurate computational results for this system, we use a variant of the geometrical cluster algorithm (GCA) [22]. This is a sophisticated Monte Carlo scheme that samples the Boltzmann distribution of a system by updating large groups ("clusters") of particles, with both colloids and depletants moving together. Use of such a specialized technique is essential for coping with the disparity in size between colloids and depletant. Standard Monte Carlo and Molecular Dynamics techniques are unequal to the task of relaxing such systems because the depletant acts to frustrate colloidal motion except on very small length scales. This problem can be readily appreciated from Fig. 1.

The GCA is based on self-inverse geometric operations that can be tailored to effectively sample the system of interest. In the case of self-assembled structures it is essential that relaxation occurs on all length scales to ensure ergodicity. To this end we use the combination of updates described in Fig. 2: A "pivot" (point reflection) operation (see Fig. 2(a)) is employed to relax particle positions, while a plane reflection operation [23] allows colloids to sample different orientations. For the latter operation, if the reflection plane is constrained to lie close to the orientation vector of a monomer in the chain, then this monomer samples small variations in position and orientation within its binding pocket (Fig. 2(b)). On the other hand, if the plane is placed through the center of the monomer at an arbitrary angle to the orientation vector, then large scale flexing of the polymer occurs (Fig. 2(c)). Pivot moves in the GCA are rejection-free by construction. However, to ensure the local character of the updates shown in Fig. 2(b), we reject moves in which the colloid in its new position overlaps with a second colloid. For the move of Fig. 2(c) we ensure consistency with periodic boundary conditions by rejecting the proposed update if the linear dimension of the cluster exceeds half the box size. All updates exploit a highly efficient hierarchical overlap search algorithm that allows us to determine whether a proposed move leads to overlaps of our anisotropic particles [24–26].

The depletant particles are treated grand-canonically in our simulations. That is, their number is free to fluctuate, corresponding to the common experimental situation of a depletant that is in equilibrium with a bulk reservoir. We therefore quote the depletant reservoir volume fraction $\eta_s^r = N_s\pi\sigma_s^3/(6V)$ as a measure of the driving force for depletion induced assembly, where N_s is the average number of depletant particles.

Turning to our simulation results, we first assess how

the degree of polymerization depends on the depletant volume fraction η_s^r. To this end, we label the indentation on each colloidal particle as its "lock site". The concave part of the surface acts as the "key", which fits snugly in the lock. Let $N_{\rm L}$ be the average number of lock sites that are available for binding (where no other colloidal particle is already bound), and let $N_{\rm K}$ be the average number of colloidal particles that are not currently occupying any lock site (occupation of a lock site is decided on the basis of a radial cutoff criterion; results are insensitive to the choice of this cutoff). The number densities of such particles are then $\rho_{\rm L} = N_{\rm L}/V$ and $\rho_{\rm K} = N_{\rm K}/V$. We also define $X = \rho_{\rm L}/\rho$. For an unassociated fluid, $X \approx 1$; for a system consisting of long colloidal polymers then $X \approx 0$. If the polymers are 'tree-like' (without closed loops), then the average degree of polymerization is $1/X$.

Fig. 3(a) depicts our measurements of X (black circles) for various h, as the depletant volume fraction η_s^r is increased. The range of η_s^r over which polymerization occurs is quite narrow in each case (particularly for deep indentations), and this range is shifted to smaller η_s^r as h increases. Physically, the lock-and-key binding is strongest when the colloid indentations are deep, and the shape complementarity is most pronounced. At the largest values of η_s, almost all the colloids are members of chains, $X \approx 0$.

Fig. 4 shows snapshots of the equilibrated polymer configurations that form for $h = 0.5$ and $h = 0.3$, at values of η_s^r corresponding to $X \approx 0.1$. Compared with the results for $h = 0.7$ (Fig. 1) one observes that deeper indentations result in stiffer chain conformations. To quantify these differences, we have measured the persistence length b, defined through $\langle \cos(\theta_L) \rangle = e^{-L/b}$, where θ_L is the angle between orientation vectors of colloid particles that are Lth neighbours in the chain. Thus, large values of b correspond to stiff chains: for $h = (0.3, 0.5, 0.7)$, we find $b = (1.0, 3.3, 9.1)\sigma_l$. This wide range of b illustrates how the properties of self-assembled colloidal polymers may be controlled through the colloid shape.

For shallower indentations the assembled polymers may support branching. This is only possible when the indentation is small enough for two colloid particles to "lock onto" the convex part of a third one. The marginal case is $h = 0.5$, for which a single key surface can just accommodate two locks. As h decreases, the branching probability increases rapidly. When bonds are strong ($X < 0.1$ as in Fig. 4), we find that the fractions of particles involved in branching for $h = (0.5, 0.4, 0.3)$ are $(1\%, 9\%, 15\%)$. Again, by changing the colloid shape, the self-assembled chains can be varied from linear polymers ($h = 0.7$) to chains with a few branches ($h = 0.5$), and finally ($h = 0.3$) to strongly branched structures reminiscent of the network fluid (or "empty liquid") states found in studies of "patchy" colloids [15, 16].

Given that this range of behaviour is possible on varying just the depletant density η_s^r and the indentation depth h, theoretical insight is very valuable in guiding choices of colloidal geometry and depletant parameters, both in simulation and, potentially, in experiment. We have applied Wertheim's theory of associating fluids [27] to these indented colloids, following the work of Sciortino and co-workers [15, 28] on 'patchy' colloids. This theory generalizes liquid state theory, incorporating steric constraints. For example, at most one particle may occupy any lock site; we also assume that chain branching may not occur, which is valid for $h \gtrsim 0.5$. Within the theory, depletion interactions appear as two-body effective interactions between the colloidal particles, obtained formally by integrating out the depletant fluid. Based on these assumptions, Wertheim's theory gives a diagrammatic series for the density functional of the system, from which the number densities $\rho_{\rm L}$ and $\rho_{\rm K}$ may be derived.

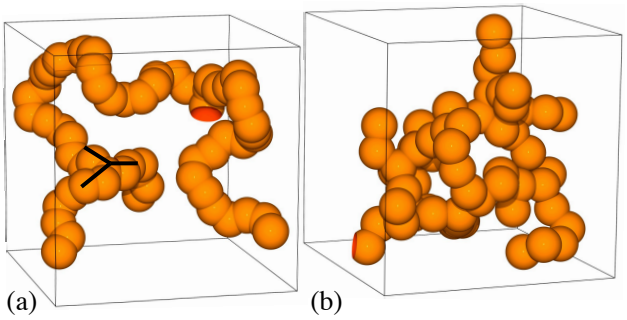

FIG. 4: (Color online) Snapshots for $X < 0.1$ (depletant not shown) and varying indentation depth. **(a)** At $h = 0.5$, $\eta_s^r = 0.105$, this system consists of just two large chains. A single branch point is also indicated. **(b)** At $h = 0.3$, $\eta_s^r = 0.14$, the polymers form an interconnected network of chains, reminiscent of an empty liquid [15].

At leading order, the theory reduces to the familiar law of mass action: $\rho_{\rm LK} = \rho_{\rm L}\rho_{\rm K}K_0$ where $\rho_{\rm LK} = \rho - \rho_{\rm L}$ is the number density of bonds (i.e. the number density of occupied lock sites), and K_0 is the bare equilibrium constant, which depends on the attractive forces between particles. The law of mass action applies quite accurately in the dilute limit $\rho\sigma_l^3 \ll 1$, but to go beyond this limit, one must also take account of repulsive forces between particles, and the resulting packing effects. The second part of Wertheim's theory achieves this by a perturbative expansion about a reference system without any attractive interactions ($\eta_s^r = 0$). The theory is therefore accurate if the packing of particles in the presence of attractive forces is very similar to their packing in the reference system. Formally, the thermodynamic perturbation theory (TPT) of Wertheim approximates the density functional of the system by an infinite subset of terms in its diagrammatic expansion. The result is that the bare equilibrium constant K_0 in the law of mass action is replaced by [28]

$$K = \frac{1}{\Omega} \int {\rm d}\boldsymbol{r}_{12}\, {\rm d}\boldsymbol{\omega}_2\, g_{\rm R}(\boldsymbol{r}_{12}, \boldsymbol{\omega}_1, \boldsymbol{\omega}_2) f_{\rm A}(\boldsymbol{r}_{12}, \boldsymbol{\omega}_1, \boldsymbol{\omega}_2). \quad (1)$$

Here $\boldsymbol{\omega}_1, \boldsymbol{\omega}_2$ represent the orientations of two particles, with $\boldsymbol{r}_{12}$ the vector between them, and Ω is the phase space volume associated with one particle's orientation. Also, $g_{\rm R}(\boldsymbol{r}, \boldsymbol{\omega}_1, \boldsymbol{\omega}_2)$ is the two-particle distribution function in the reference system (without attractions), while $f_{\rm A}(\boldsymbol{r}, \boldsymbol{\omega}_1, \boldsymbol{\omega}_2)$ is a Mayer-f function associated with the attractive part of the effective interactions between particles. In the dilute limit, $g_{\rm R} = 1$ except when the two particles overlap, and one recovers the standard formula for the bare equilibrium constant $K = K_0$. Outside the dilute regime, particle packing effects are taken account of through $g_{\rm R}$.

For the spherical patchy particles considered by Sciortino and co-workers [28], $g_{\rm R}$ can be approximated from Percus-Yevick theory, and $f_{\rm A}$ is known exactly. Thus, the TPT calculation can be performed analytically, it describes their data very accurately. For indented colloids, neither $g_{\rm R}$ nor $f_{\rm A}$ is known exactly, but $g_{\rm R}$ may be obtained from a simulation of the reference system of indented colloids in the absence of depletant, and $f_{\rm A}$ from a simulation of two particles in the presence of depletant. The integral in (1) can then be calculated. The resulting TPT predictions are shown in Fig. 3(b) and (c) for $h = 0.7$ and $h = 0.5$ respectively: the agreement is reasonable but there are significant deviations. We attribute these deviations to differences in the packing properties of chains of particles, compared to isolated monomers. (We have ruled out the alternative possibility that many body colloidal interactions are responsible by simulating indented colloids with prescribed two-body attractive interactions, for which similar deviations from TPT are found [29].) To explore packing effects, we return to the diagrammatic analysis of Wertheim, but instead of following the TPT, we consider just a few simple terms in the density functional: see Fig. 5. Under this approximation, the law of mass action is replaced by

$$\rho_{\rm LK} = \rho_{\rm L}\rho_{\rm K}K_0[1 + \rho v_1 + \rho_{\rm LK} v_2]. \qquad (2)$$

Here, v_1 and v_2 are geometrical factors (independent of η_s^r) that account for packing of free particles and short chains: the relevant liquid-state diagrams are shown in Fig. 5. Within Wertheim's TPT, the v_1-term is included, but the v_2-term is absent. Further, comparison between (2) and the law of mass action shows that the effective equilibrium constant $\rho_{\rm LK}/(\rho_{\rm L}\rho_{\rm K})$ now depends on the degree of polymerization of the system, via the v_2-term. This constant (and hence the quantity X) must therefore be determined self-consistently by solving (2), so we refer to the analysis in the presence of the v_2-term as self-consistent Wertheim (SCW) theory.

We have obtained values for v_1 and v_2 by simulating very small systems (up to 4 indented particles, without depletant). Results are shown in Fig. 5(e). Using these values in (2) leads to the SCW predictions shown in Fig. 3. In terms of the density functional, SCW theory is a much cruder approximation than TPT. However, the SCW theory performs significantly better than TPT, accounting for around half of the deviation between theory and simulation.

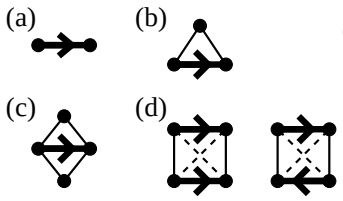

(e)

h	v_1	v_2
0.0	1.30	-0.10
0.3	1.91	-1.05
0.5	2.20	-1.34
0.7	2.35	-1.60

FIG. 5: Liquid state theory diagrams showing contributions to the density functional that are relevant for calculating $\rho_{\rm LK}$ within Wertheim theory. Directed heavy lines correspond to attractive lock-and-key binding while thin lines correspond to repulsive interactions. Where diagrams include dashed lines, this indicates a sum over diagrams both with and without these repulsive interactions. Vertices have weights corresponding to various combinations of $\rho, \rho_{\rm L}, \rho_{\rm K}$, as prescribed by Wertheim's theory. (a) Diagram for K_0; (b) Diagram for the v_1-term in (2); (c) A diagram included in the TPT but not in SCW; (d) Diagrams for the v_2-term in Eq. (2), included in SCW theory but not in TPT. The terms in (a,b,d) are those considered in the SCW theory. (e) Table showing values of v_1 and v_2 for various h, in units having $\sigma_l = 1$.

The origin of this effect is the v_2-term in (2). Physically, the v_1-term in that equation (included in both TPT and SCW theories) reflects the increased virial pressure in the system as the colloid number density increases, and enhances polymerization. The v_2-term reflects differences in packing properties between free particles and assembled chains. We find $v_2 < 0$, indicating that as polymerization occurs, the virial pressure is reduced (compared with TPT), suppressing further chain formation. For spherical patchy particles ($h = 0$), Fig. 5(e) shows that the magnitude of v_2 is small, consistent with the success of TPT in that case [28]. However, the size of v_2 grows as h is increased, leading to the deviations from TPT shown in Fig. 3. The SCW theory accounts for some of these deviations, although agreement is still not perfect. One could improve the theory by including further terms in the approximate density functional, but our main point here is that packing effects of non-spherical particles can significantly affect self-assembly, and are required for quanitative theoretical analysis.

To summarize, the sophisticated Monte Carlo techniques that we have applied here show that indented colloids can assemble into chains, with persistence lengths and branching properties controlled by a combination of colloid shape and depletant density. Two variants of Wertheim's theory have been analysed, showing how particle shapes can influence their self-assembly. Given that depletant parameters and the shapes of indented colloids can both be controlled in experiments [5, 6, 17–20], we hope that these results will stimulate further experimental studies of self-assembly in these systems.

We thank Dirk Aarts, Sam Ivell and Clement Law for helpful discussions. We are grateful to the EPSRC for funding through grant EP/I036192 (for DJA and NBW) and EP/I003797/1 (for RLJ).

[1] G. M. Whitesides and B. Grzybowski, Science **295**, 2418 (2002).
[2] S.C. Glotzer and M.J. Solomon, Nature Mat. **6**, 557 (2007).
[3] D. Nykypanchuk, M. M. Maye, D. van der Lelie and O. Gang, Nature **451**, 459 (2008).
[4] Q. Chen, S. C. Bae and S. Granick, Nature **469**, 381 (2011)
[5] L. Rossi, S. Sacanna, W. T. M. Irvine, *et al.*, Soft Matter, 7, 4139 (2011).
[6] S. Sacanna, W. T. M. Irvine, P. M. Chaikin, and D. J. Pine, Nature **464**, 575 (2010).
[7] M. Marechal, R. J. Kortschot, A. H. Demirös, A. Imhof and M. Dijkstra, Nano Lett. **10**, 1907 (2010)
[8] J. Henzie, M. Grünewald, A. Widmer-Cooper, P. L. Geissler and P. Yang, Nature Mat. **11**, 131 (2012).
[9] W. Qi, J. de Graaf, F. Qiao, S. Marras, L. Manna and M. Dijkstra, Nano Lett. **12**, 5299 (2012).
[10] P. F. Damasceno, M. Engel and S. C. Glotzer, Science, **337**, 453 (2012)
[11] G. Odriozola, F. Jimenez-Angeles, and M. Lozada- Cassou, J. Chem. Phys. **129**, 111101 (2008); Phys. Rev. Lett. **110**, 105701 (2013).
[12] S. Torquato and Y. Jiao, Nature **460**, 876 (2009)
[13] H. N. W. Lekkerkerker and R. Tuinier, *Colloids and the Depletion Interactions*, Vol. 833 of Lecture Notes in Physics (Springer, Berlin / Heidelberg, 2011).
[14] P.-M. König, R. Roth, and S. Dietrich, EPL **84**, 68006 (2008).
[15] E. Bianchi, J. Largo, P. Tartaglia, E. Zaccarelli and F. Sciortino, Phys. Rev. Lett. **97**, 168301 (2006).
[16] B. Ruzicka *et al.*, Nature Mat. **10**, 56 (2011).
[17] S. Sacanna, W. T. M. Irvine, L. Rossi and D. J. Pine, Soft Matter, **7**, 1631 (2011)
[18] J. Bahadur *et al.*, Langmuir **28**, 1914 (2012).
[19] A. M. Alsayed, Z. Dogic and A. G. Yodh, Phys. Rev. Lett. **93**, 057801 (2004)
[20] J. R. Savage and A. D. Dinsmore, Phys. Rev. Lett. **102**, 198302 (2009).
[21] D. Klotsa and R. L. Jack, J. Chem. Phys. **138**, 094502 (2013).
[22] J. Liu and E. Luijten, Phys. Rev. Lett. **92**, 035504 (2004).
[23] D. W. Sinkovits, S. A. Barr, and E. Luijten, J. Chem. Phys. **136**, 144111 (2012).
[24] M. Marechal and M. Dijkstra, Phys. Rev. E **82**, 031405 (2010).
[25] M. He and P. Siders, J. Phys. Chem. **94**, 7280 (1990).
[26] G. Cinacchi and J. S. van Duijneveldt, J. Phys. Chem. Lett. 1, **787** (2010).
[27] M. S. Wertheim, J. Stat. Phys. **35**, 19 (1984); **35**, 35 (1984); **42**, 459 (1986); **42**, 477 (1986).
[28] F. Sciortino, E. Bianchi, J. F. Douglas, and P. Tartaglia, J. Chem. Phys. **126**, 194903 (2007).
[29] D. J. Ashton, R. L. Jack and N. B. Wilding, in preparation.